Temporal and spatial variabilities in surface mass balance at the EGRIP site, Greenland from 2009 to 2017

Yuki Komuro [a],[*], Fumio Nakazawa [a],[b], Motohiro Hirabayashi [a], Kumiko Goto-Azuma [a],[b], Naoko Nagatsuka [a], Wataru Shigeyama [a],[b], Sumito Matoba [c], Tomoyuki Homma [d], Jørgen Peder Steffensen [e], Dorthe Dahl-Jensen [e]

[a] National Institute of Polar Research, 10-3 Midori-cho, Tachikawa, Tokyo, 190-8518, Japan
[b] The Graduate University for Advanced Studies, SOKENDAI, Shonan Village, Hayama, Kanagawa, 240-0193, Japan
[c] Institute of Low Temperature Science, Hokkaido University, Sapporo, 060-0819, Japan
[d] Nagaoka University of Technology, Nagaoka, Niigata, 940-2188, Japan
[e] Physics of Ice Climate and Earth, Niels Bohr Institute, University of Copenhagen, Tagensvej 16, DK-2200, Copenhagen N, Denmark

ARTICLE INFO

ABSTRACT

Temporal variability in surface mass balance (SMB) on the Greenland ice sheet is important for understanding the mass balance of the ice sheet. Additionally, knowledge of the spatial variability in SMB at ice core drilling sites helps to interpret the spatial representativeness of SMB data obtained from a single ice core. In this study, to investigate the spatiotemporal variability in recent SMB in the East Greenland Ice Core Project (EGRIP) area in the northeastern Greenland ice sheet, pit observations were made at six sites in the summers of 2016–2018. In all pits, depth profiles of water isotope ratios showed clear seasonal variations. The annual SMB differed from site to site, which is probably due to post-depositional redistribution of snow caused by wind erosion and snowdrift. However, the multiple-site averages of annual SMBs, which ranged from 134 to 157 mm w. e. yr^{-1} (average 146 mm w. e. yr^{-1}) during 2009–2017, were very similar. This indicates that annual SMBs in the EGRIP area were nearly constant in this period. The seasonal SMBs in the EGRIP area tended to be larger in the summer–winter period than in the winter–summer period.

1. Introduction

The mass loss of the Greenland ice sheet is accelerating due to the effects of climate change (e.g., Rignot et al., 2011; Shepherd et al., 2012). Surface mass balance (SMB) is one of the main factors controlling the total mass balance of the ice sheet. The SMB varies across the Greenland ice sheet due to the effects of meteorological conditions, as well as the topographic effects of the ice sheet (Ohmura and Reeh, 1991; Bales et al., 2001).

Present SMB on the Greenland ice sheet is observed using snow stakes and automatic snow depth gauges (e.g., Steffen and Box, 2001; Castellani et al., 2015). Additionally, snow pits, ice cores, and ground-penetrating radar are used to investigate past SMB (e.g., Anklin and Stauffer, 1994; Fischer et al., 1998a,b; Hawley et al., 2014). These *in situ* observation data are needed to validate polar regional climate models (e.g., Noël et al., 2015; Fettweis et al., 2017; Langen et al., 2017;

Niwano et al., 2018), which have been used to estimate spatiotemporal variability in snowfall as well as its resultant ice-sheet-wide SMB. However, although a large number of *in situ* observations have been made, these observation data do not cover a sufficient geographical area or period of time (e.g., Bales et al., 2001; Koyama and Stroeve, 2019). In particular, there are fewer *in situ* observations in northeastern Greenland compared with other areas of the ice sheet.

Previous studies suggested the possibility that precipitation in the Arctic has recently increased because of an enhanced moisture supply due to global warming and the retreat of Arctic sea ice (e.g., Zhang et al., 2013; Kopec et al., 2016). The retreat of Arctic sea ice might have led to enhanced evaporation from the Arctic Sea, thereby increasing local precipitation (Kopec et al., 2016). In the 21st century, the increasing rate of precipitation caused by environmental changes and increased moisture supply is predicted to be higher in northeastern Greenland than in other areas of the ice sheet (Bintanja and Selten, 2014). Additionally,

---

the increase in precipitation is predicted to occur primarily during the summer–winter period (Bintanja and Selten, 2014). The variation in SMB in a given area of the Greenland ice sheet reflects the variation in precipitation there. Understanding the recent SMB in the northeastern Greenland is essential for discussing the total ice sheet mass balance. In addition, SMB data with seasonal resolution are required to elucidate the relationship between the SMB and changes in the climate/environment.

However, surface snow on the Greenland ice sheet can be redistributed by wind erosion and snowdrifts, which are dependent on near-surface wind speed and snow surface grain shape. Thus, to understand the areal average of SMB in a specific year or season, multi-site observation is preferable. In particular, the proportion of redistributed snow is expected to be relatively large in the lower accumulation area. Northeastern Greenland is one of the lowest accumulation areas in Greenland (Ohmura and Reeh, 1991), and thus multi-site observation is particularly important in this area. Moreover, multi-site observational data can be used to investigate the spatial variability in SMB, which is necessary for interpreting the spatial representativeness of SMB data obtained from a single ice core (e.g., Gfeller et al., 2014).

In 2015, the East Greenland Ice Core Project (EGRIP)—the first deep coring project in East Greenland—was launched by an international team led by the University of Copenhagen, Denmark. This project aims to study the Holocene paleoclimate with a high temporal resolution as well as the ice dynamics of the Greenland ice sheet. We have been participating in EGRIP under the Arctic Challenge for Sustainability (ArCS) and Arctic Challenge for Sustainability II (ArCSII) projects. One of the purposes of the ArCS projects is to investigate recent SMB in the EGRIP area.

Our other study reports variation in recent annual SMB as well as the seasonality of snow chemistry based on observations from two pits conducted at EGRIP in 2016 (Nakazawa et al., this issue). We found a substantial increase in recent annual SMB in this area, as much as 50% compared with the average for the period 1607–2011 (Vallelonga et al., 2014). However, to better understand the spatial average and variability in SMB, it is necessary to make observations at more sites in the EGRIP area. In addition, the obtained results provide robust evidence for the increasing trend of SMB in recent years. Furthermore, information about the spatial variability in SMB in the EGRIP area allows for an accurate interpretation of the ice core data obtained from this area.

In this study, we aim to (1) clarify the spatial variation in SMB. The obtained results should be useful for assessing the spatial representativeness of SMB data obtained from a single ice core in this area as well as for validating the satellite observation data. We also aim to (2) elucidate recent temporal variations in SMB in the EGRIP area and (3) examine the recent seasonal variations in SMB in the EGRIP area to determine possible factors affecting temporal SMB variations. To achieve these aims, we conducted pit observations at six sites around the EGRIP camp during the summers of 2016–2018. For the first aim, we investigated the site-to-site difference in SMB in the EGRIP area, and compared the SMB obtained for each site with the average SMB across multiple sites. For the second aim, we used pit data from six sites to estimate annual and seasonal SMB as areal averages in the EGRIP area over the past eight years, and compared our results with those obtained for other parts of Greenland in previous studies. For the third aim, we investigated the seasonality of SMB in the EGRIP area.

2. Study area and methods

In the summers of 2016–2018, pit observations were conducted at six sites around the EGRIP camp (Fig. 1, Table 1; 75.6299°N, 35.9937°W, 2720 m a.s.l.). Observations were made at two sites (Pit 1 and Pit 2) in

Table 1
Snow pits characteristics.

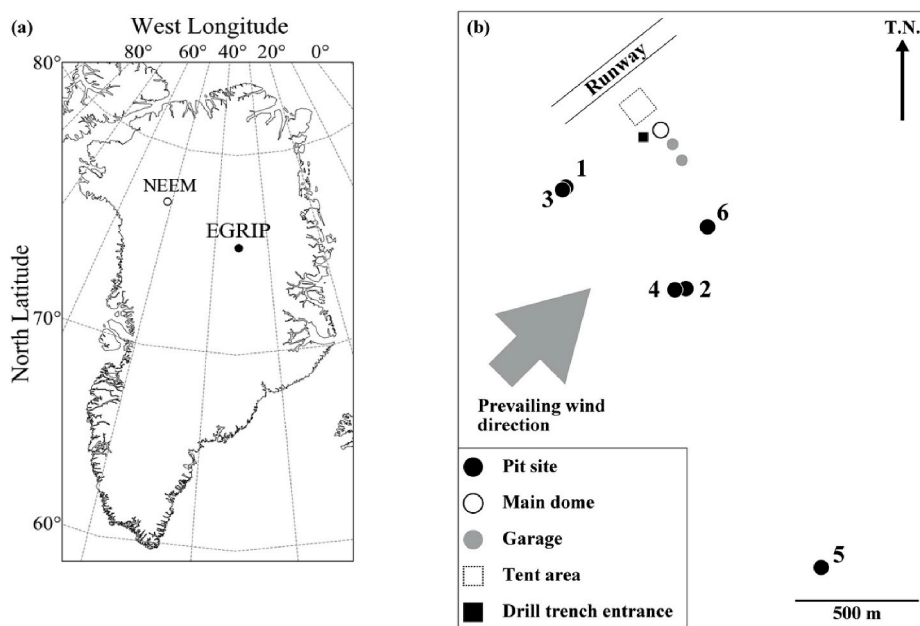|	Observation date (yyyy/mm/dd)	Depth (m)	Period covered	Latitude (°N)	Longitude (°W)
Pit 1	2016/6/29–2016/7/5	4.02	2006–2016	75.6289	36.0039
Pit 2	2016/7/11–2016/7/12	3.18	2009–2016	75.6252	35.9860
Pit 3	2017/6/13	2.01	2013–2017	75.6288	36.0045
Pit 4	2017/6/16	2.01	2013–2017	75.6252	35.9876
Pit 5	2017/8/6–2017/8/8	2.22	2012–2017	75.6150	35.9658
Pit 6	2018/7/3–2018/7/5	2.01	2014–2018	75.6275	35.9828

Fig. 1. (a) Map of the study area. EGRIP, East Greenland Ice Core Project (this study); NEEM, North Greenland Eemian Ice Drilling (a previous deep drilling site). (b) Locations of the pit observation sites and camp facilities in EGRIP; 'Main dome' denotes the main building of the camp, which is located at 75.6299°N, 35.9937°W.

2016, three sites (Pit 3, Pit 4, and Pit 5) in 2017, and one site (Pit 6) in 2018. We also used the data from Pit 1 and 2 reported by Nakazawa et al., (2020). The location and depth of each pit are shown in Fig. 1 and Table 1. In all pits, snow samples for the measurement of snow density and stable water isotope ratios ($\delta^{18}O$ and δD) were collected at 0.03-m intervals from the snow surface to the bottom of the pits. To measure snow density, snow blocks were taken from pits using a snow sampler with a volume of 100 cm^3. We inserted the sampler horizontally into the pit wall and removed a block of snow. Then, the snow block was weighed. Measurement error in density occurs when the block of snow is removed and weighed. The density measurement error is estimated to be

within 5%, which is considered to be due mainly to the measurement error in volume because that of the weight measurement is less than 1%. Samples for water isotope analyses were taken using a plastic spatula and a ceramic knife, both of which were pre-cleaned. Each sample collected for water isotope analyses was placed in a dust-free plastic bag for Pits 1–5 and a pre-cleaned polysulfone cup for Pit 6. The samples collected from Pits 1–4 were melted in the plastic bags and then transferred to pre-cleaned polypropylene bottles and re-frozen in the EGRIP camp. The samples collected from Pits 5 and 6 were kept frozen in the plastic bags or cups in the EGRIP camp. All samples were transported to the National Institute of Polar Research in a frozen state. Then, the
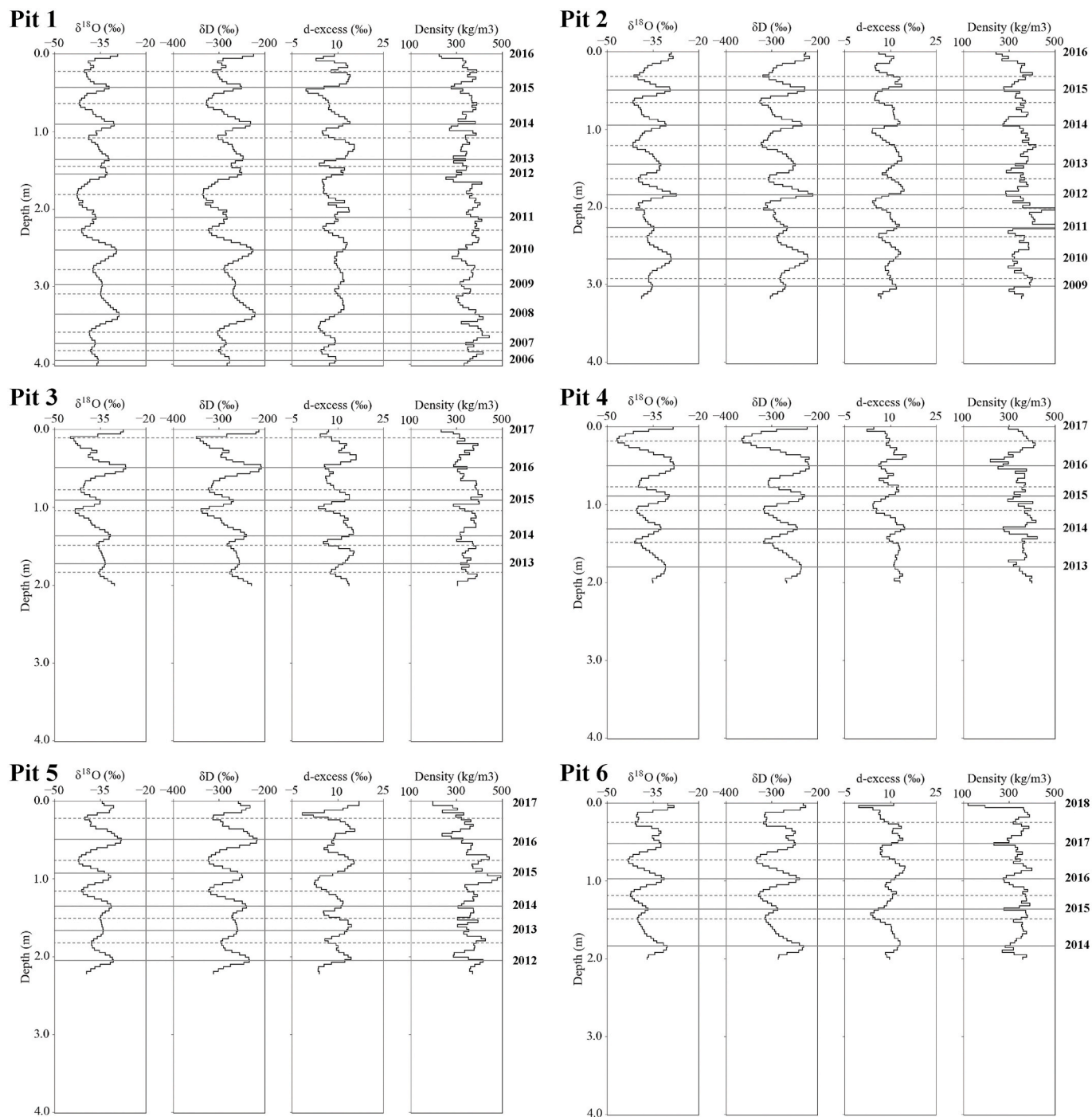

Fig. 2. Depth profiles of $\delta^{18}O$, δD, deuterium excess (d-excess), and snow density for six pits. The profiles for Pit 1 and Pit 2 are the results reported by Nakazawa et al., (2020) and the profiles for Pits 3–6 are the results from the present study. In each profile, the solid gray and dotted lines show the summer and winter layers, respectively. The year beside each solid gray line indicates the summer of that year.

samples were melted in a laboratory and used for measurements of stable water isotope ratios. The $\delta^{18}O$ and δD values were measured with a dual-inlet mass spectrometer (Thermo Fisher Scientific, Delta V) using an equilibrium method (Uemura et al., 2004). The precision (1σ) of determination was 0.05‰ for $\delta^{18}O$ and 0.5‰ for δD (Uemura et al., 2004).

3. Results and discussion

3.1. Seasonal variations of water isotope ratios and snow density

Fig. 2 shows the depth profiles of stable water isotope ratios, deuterium excess (d-excess; d = δD − 8 × $\delta^{18}O$), and snow density obtained from all pits. The profiles of Pits 3–6 showed the same periodic patterns reflecting seasonal variation as Pits 1 and 2 (Nakazawa et al., this issue). The profiles of $\delta^{18}O$ showed in-phase variation with those of δD. The profiles of d-excess showed periodic patterns, which were out of phase with the profiles of $\delta^{18}O$ and δD. The snow density tended to vary inversely with $\delta^{18}O$ and δD.

Previous studies at other sites in Greenland reported seasonality of $\delta^{18}O$ is related to the air temperature at the time when the snow was deposited, with $\delta^{18}O$ reaching a maximum in summer and a minimum in winter (Johnsen et al., 1972; Dansgaard, 1973; Steffensen, 1985; Finkel et al., 1986; Beer et al., 1991; Legrand and Mayewski, 1997; Kuramoto et al., 2011). It is also known that d-excess reflects the evaporation environment on the sea surface in the source area of the water vapor that caused the snowfall (Uemura, 2007). Previous studies in Greenland reported that d-excess presented a minimum from spring to early summer, and a maximum in autumn (Johnsen et al., 1989; Kuramoto et al., 2011). Pits 1 and 2 were dated using the seasonal variations of $\delta^{18}O$, δD, and d-excess, as well as the annual peaks of methanesulfonic acid appearing from summer to autumn (Nakazawa et al., this issue). The depth profiles of $\delta^{18}O$ and d-excess in Pits 3–6 showed clear seasonal variations, as did those of Pits 1 and 2. Therefore, in this study we dated Pits 3–6 using the seasonal variations of $\delta^{18}O$ and d-excess.

The ages determined for Pits 3–6 are shown in Fig. 2. Dating based on seasonal variations of $\delta^{18}O$ and d-excess indicated that Pits 3 and 4 cover four years between 2013 and 2017, Pit 5 covers five years between 2012 and 2017, and Pit 6 covers four years between 2014 and 2018. Pit 6 has two peaks of $\delta^{18}O$ between depths of 0.36–0.39 m and 0.51–0.54 m. The snow density has a minimum at the peak at 0.51–0.54 m depth and a maximum at the peak at around 0.36–0.39 m depth. Thus, we took the depth of 0.51–0.54 m to represent the summer layer in 2017.

3.2. Annual surface mass balance

Fig. 3 shows the variation in annual SMB in the six pits. Annual SMBs and multiple-year averages in the pits are shown in Table 2. We defined the period from one summer to the next as a mass balance year. The annual SMB at Pits 3 and 4 for 2013–2017 varied from 123 to 159 and 133–177 mm water equivalent (w.e.) yr^{-1}, respectively, while the average at these two pits during this period were 148 and 157 mm w. e. yr^{-1}, respectively. The annual SMB at Pit 5 for 2012–2017 varied from 104 to 184 mm w. e. yr^{-1} and averaged 144 mm w. e. yr^{-1}. The annual SMB at Pit 6 for 2014–2018 varied from 134 to 168 mm w. e. yr^{-1} and averaged 154 mm w. e. yr^{-1}.

The multiple-site averages of annual SMBs were calculated using SMB data from the six pits (Table 2). For the common period 2013–2017, their variations were small, ranging from 147 to 157 mm w. e. yr^{-1} (average 152 mm w. e. yr^{-1}). However, for the period 2009–2017, they showed larger variability, ranging from 110 to 187 mm w. e. yr^{-1} (average 148 mm w. e. yr^{-1}). Their relative standard deviations for the period 2009–2017 (14.7%) was larger than that for the period 2013–2017 (3.3%). The layers of 2011–2012 and 2012–2013 in Pits 1 and 2 were affected by snow melting and re-freezing due to the surface melting in summer 2012 (Nakazawa et al., in this issue).
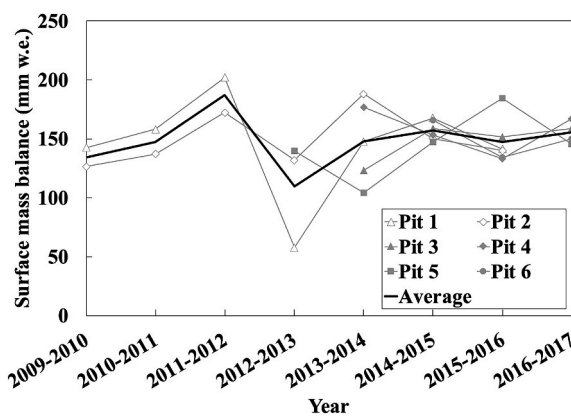

Fig. 3. Variations in annual SMBs. The gray lines show the annual SMBs for each pit and the black line shows the multiple-site average SMB calculated from the multi-pit data. The ranges on the x-axis indicate the period from one summer to the next (e.g., 2009–2010 means the period from the summer of 2009 to the summer of 2010).

Additionally, in Pit 5, inhomogeneous ice layers were observed in the summer layer of 2012 (at approximately 2.05 m depth). Therefore, the multiple-site average SMBs for 2011–2012 and 2012–2013 were averaged and the average for 2011–2013 was calculated to remove the effect of water redistribution due to snow melting and refreezing. For this process, we used data from only Pits 1 and 2 because there was no data for Pit 5 during 2011–2012. The average SMB for 2011–2013 was 141 mm w. e. yr^{-1}, and the multiple-site average SMBs for 2009–2017 ranged from 134 to 157 mm w. e. yr^{-1} (average 146 mm w. e. yr^{-1}). According to this two-year averaging procedure, the variability in multiple-site average SMBs in 2009–2017 was smaller.

Although the annual SMBs for 2009–2017 differed from site to site, the multiple-site average SMBs for different years were very similar. The relative standard deviations of the annual SMBs for 2009–2017 ranged from 5.3% to 41.2%, which are larger than the density measurement error (≤5%). The similarity between the multiple-site average SMBs for different years between 2009 and 2017 indicates that annual SMBs as areal averages in the EGRIP area were nearly constant in this period. Additionally, the five- and seven-year averages of the annual SMBs for each pit is consistent with those calculated from the multi-pit data in the same period. The five-year average of annual SMBs for Pit 5 in 2012–2017 is consistent with the five-year average of the multiple-site average SMBs in this period (144 mm w. e. yr^{-1}). The seven-year averages of annual SMBs for Pits 1 and 2 in 2009–2016 (145 and 149 mm w. e. yr^{-1}, respectively) are very close to the seven-year average of the multiple-site average SMBs in this period (147 mm w. e. yr^{-1}). This closeness indicates that the 5–7 year average of annual SMBs at one site can be used as an areal average SMB in the EGRIP area.

To estimate the effect of the post-depositional redistribution of snow on the annual SMB in the EGRIP area, the spatial variability in SMB for each year (V) was calculated using the following equation:

$$V = \frac{B_{pit}}{B_{ave}} \times 100 \tag{1}$$

where B_{pit} is the annual SMB in an arbitrary year obtained from each pit, and B_{ave} is the multiple-site average of the annual SMBs in the same year. The V values for 2009–2017 ranged between 53% and 127%, with the maximum and minimum values both being observed for the 2012–2013 SMB. Excluding the 2011–2012 and 2012–2013 SMBs, which were affected by snow melting and refreezing, the minimum and maximum V values in 2013–2014 were 71% and 127%, respectively. This indicates that single-site observation in the EGRIP area can provide SMBs for each year, including a maximum ±30% uncertainty from those multiple-site averages without the effects of surface melting and re-

Table 2

Annual SMBs (mm water equivalent) for the six pits. The average of annual SMBs for the period covered by each pit is shown in the bottom row of the table. The multiple-site average of annual SMBs is shown in the column on the far right.

Period	Pit 1	Pit 2	Pit 3	Pit 4	Pit 5	Pit 6	Multiple-site average ± SD
Summer 2017 to summer 2018						168	
Summer 2016 to summer 2017			159	167	146	150	155 ± 9
Summer 2015 to summer 2016	141	140	152	133	184	134	147 ± 19
Summer 2014 to summer 2015	168	150	159	153	147	166	157 ± 8
Summer 2013 to summer 2014	148	188	123	177	104		148 ± 35
Summer 2012 to summer 2013	58	132			140		110 ± 45 (141)
Summer 2011 to summer 2012	202	172					187 ± 21 (141)
Summer 2010 to summer 2011	158	137					148 ± 15
Summer 2009 to summer 2010	143	126					134 ± 11
Average of annual SMBs ± SD	145 ± 44	149 ± 23	148 ± 17	157 ± 19	144 ± 28	154 ± 16	148 ± 22[a] 146 ± 8[b]

SD, standard deviation. The values in parentheses are based on the two-year average of SMBs for 2011–2013 from Pits 1 and 2.

[a] Eight-year average of multiple-site averages for 2009–2017.

[b] Eight-year average of multiple-site averages calculated using the values in parentheses.

freezing.

In this study, the multiple-site averages of annual SMBs for 2009–2017 (134–157 mm w. e. yr^{-1}) are consistently higher than the average for 1607–2011 (0.10 m w. e. yr^{-1}). Additionally, the eight-year average of the multiple-site averages for 2009–2017 (146 mm w. e. yr^{-1}) is approximately 50% higher than the average for 1607–2011. Our results provide additional robust evidence for the recent increase in SMB in the EGRIP area, confirming the result of Nakazawa et al. (this issue).

3.3. Seasonal surface mass balance

To investigate the seasonality of SMB in the EGRIP area, we divided each year into two periods—the half-year period from summer to winter (summer–winter) and the half-year period from winter to summer (winter–summer)—and compared the SMBs for each period.

Table 3 shows the half-year SMBs in the six pits, as well as the multiple-year and multiple-site averages. The multiple-year averages during the summer–winter period were higher than those during the winter–summer period. For each year, the multiple-site averages of

Table 3

Seasonal SMBs (mm water equivalent) for the six pits. The average of summer–winter (winter–summer) SMBs for the period covered by each pit is shown in the bottom row of the table. The multiple-site average of summer–winter and winter–summer SMBs is shown in the column on the far right.

Period	Pit 1	Pit 2	Pit 3	Pit 4	Pit 5	Pit 6	Multiple-site average ± SD
Winter 2017/18 to summer 2018						79	
Summer 2017 to winter 2017/18						89	
Winter 2016/17 to summer 2017			29	57	60	69	54 ± 17
Summer 2016 to winter 2016/17			129	109	86	81	101 ± 22
Winter 2015/16 to summer 2016	70	82	93	91	100	69	84 ± 13
Summer 2015 to winter 2015/16	72	58	58	42	84	65	63 ± 14
Winter 2014/15 to summer 2015	73	50	41	62	73	43	57 ± 14
Summer 2014 to winter 2014/15	95	100	118	91	75	123	100 ± 18
Winter 2013/14 to summer 2014	59	86	40	61	53		60 ± 17
Summer 2013 to winter 2013/14	89	102	83	115	51		88 ± 24
Winter 2012/13 to summer 2013	29	60			56		48 ± 17
Summer 2012 to winter 2012/13	29	72			83		61 ± 29
Winter 2011/12 to summer 2012	90	66					78 ± 18
Summer 2011 to winter 2011/12	111	107					109 ± 3
Winter 2010/11 to summer 2011	70	42					56 ± 20
Summer 2010 to winter 2010/11	88	95					92 ± 5
Winter 2009/10 to summer 2010	79	91					85 ± 9
Summer 2009 to winter 2009/10	64	35					50 ± 20
Average of summer-winter SMBs ± SD	78 ± 27	81 ± 27	97 ± 32	89 ± 33	76 ± 14	89 ± 24	83 ± 22[a] 82 ± 21[b]
Average of winter-	67 ± 19	68 ± 19	51 ± 29	68 ± 15	68 ± 19	65 ± 15	65 ± 15[a] 66 ± 15[b]

(continued on next page)

Table 3 (*continued*)

Period	Pit 1	Pit 2	Pit 3	Pit 4	Pit 5	Pit 6	Multiple-site average ± SD
summer SMBs ± SD							

Note: SD indicates standard deviation.
[a] Eight-year seasonal average of multiple-site averages for 2009–2017.
[b] Six-year seasonal average of multiple-site averages excluding the period during 2011–2013.

SMBs for each half-year period were calculated using SMB data from the six pits. The multiple-site average SMBs tended to be higher in the summer–winter period than in the winter–summer period; however, the opposite was true in 2015–2016 and 2009–2010. In 2009–2017, the multiple-site average SMBs during the summer–winter and winter-–summer periods ranged from 50 to 109 and 48–85 mm w. e. yr^{-1}, respectively. The eight-year multiple-site average was 83 mm w. e. yr^{-1} for summer–winter SMBs and 65 mm w. e. yr^{-1} for winter–summer SMBs. After excluding 2011–2012 and 2012–2013, which were affected by snow melting and re-freezing, the six-year multiple-site average was 82 mm w. e. yr^{-1} for summer–winter SMBs and 66 mm w. e. yr^{-1} for winter–summer SMBs.

A comparison of the eight-year average SMBs for each half-year period in 2009–2017 showed that the average for the summer–winter period was 18 mm w. e. yr^{-1} (28%) higher than that for the winter-–summer period. The variability in the multiple-site average SMBs for each half-year period in 2009–2017 was approximately 2–3 times higher than that of the multiple-site averages of annual SMBs in those years. This large variability in seasonal SMBs is due to the seasonality of SMBs in 2015–2016 and 2009–2010, which is opposite to that in the other years. However, based on the discussion in the previous section, the seasonality of SMB in the EGRIP area may not significantly affect annual SMBs.

Kuramoto et al. (2011) reported that the SMB in the North Greenland Eemian Ice Drilling (NEEM) area, located in northwestern Greenland, was larger during the winter–summer period than the summer–winter period in 2006–2008. In contrast, we found that SMB in the EGRIP area was larger during the summer–winter period.

Nusbaumer et al. (2019) reported that much of the moisture in eastern Greenland originates in the seas and ocean around Iceland, including the North Sea and the Norwegian Sea (which lie to the east of Greenland), whereas much of the moisture in western Greenland originates in the Labrador Sea area (to the southwest of Greenland). Thus, the EGRIP area, which is located in northeastern Greenland (i.e., a part of eastern Greenland), is expected to receive a large amount of water vapor from the seas to the east of Greenland; accordingly, the seasonal changes in SMB in the EGRIP area are likely to be related to the seasonal changes in moisture supply from these areas. Seasonal changes in sea surface conditions in these areas, including ice area and surface temperature, may be one of the factors contributing to the seasonality of the moisture supply to the EGRIP area. Furthermore, northeastern Greenland is expected to receive air masses from the west (e.g., Ohmura and Reeh, 1991; Buchardt et al., 2012). It has been suggested that the ice divide in the Greenland ice sheet may block water vapor transported from the west, cause precipitation in the northwestern area, and subsequently transport dry air to the northeastern area (e.g., Ohmura and Reeh, 1991). In northeastern Greenland, when the dry air supply from the west is dominant, the water vapor supply from the east can be intercepted. Thus, seasonal changes in the air masses from the west can be one of the causes of the seasonal changes in SMB in the EGRIP area. Different contributions in the transport of air masses from the west, as well as water vapor from the east, to the EGRIP and NEEM areas may explain the seasonality of SMB in those areas. In a future study, we will investigate atmospheric and sea surface conditions using resources such as

climate models, satellite observation data, and reanalysis data, to reveal the cause of temporal and seasonal SMB variation. Additionally, we analyze ice cores drilled in the EGRIP area to understand longer-term variations in SMBs in this area.

4. Summary

Between 2016 and 2018, we conducted six snow pit observations at the EGRIP area, located in northeastern Greenland, to clarify the spatial and temporal variations in SMB as well as recent seasonal variations in SMB in the EGRIP area. The results showed that the pits analyzed in this study (Pits 3–6) had clear seasonal variations in the depth profiles of δ^{18}O and d-excess, as was observed for Pits 1 and 2 in our previous study (Nakazawa et al., this issue). Based on these seasonal variations, each pit was dated, and it was found that Pits 3 and 4 cover four years between 2013 and 2017, Pit 5 covers five years between 2012 and 2017, and Pit 6 covers four years between 2014 and 2018.

We calculated annual SMB between one summer and the next in the EGRIP area using the data from Pits 1–6. The annual SMB differed among the pit sites. This difference was likely caused by post-depositional redistribution of snow due to wind erosion and snowdrift. However, the multiple-site averages of annual SMBs in 2009–2017 ranged from 134 to 157 mm w. e. yr^{-1} (average 146 mm w. e. yr^{-1}) if the data for 2011–2012 and 2012–2013 are averaged. This indicates that annual SMBs in the EGRIP area were nearly constant in 2009–2017. The average value of 146 mm w. e. yr^{-1} is approximately 50% higher than the average for 1607–2011 (Vallelonga et al., 2014). Our result confirmed the results of Nakazawa et al. (this issue).

The spatial variability in annual SMBs in the EGRIP area indicated that single-site observation in this area can provide SMBs for each year, including a maximum ±30% uncertainty from the multiple-site averages without the effects of surface melting and re-freezing. Furthermore, five- and seven-year averages of annual SMBs for each pit were consistent with those calculated from the multi-pit data in the same period. This suggests that the five-to seven-year average of annual SMBs at one site might cancel out the effect of wind erosion and snow drift, and thus could be regarded as the areal average SMB in the EGRIP area.

To obtain the seasonal SMB in the EGRIP area, we divided each year into two half-year periods, namely, summer–winter and winter-–summer, and calculated the multiple-site and multiple-year averages of SMBs for each period. In six out of the eight years between 2009 and 2017, the multiple-site average of SMBs during the summer–winter period was larger than that during the winter–summer period. The eight-year average during the summer–winter period was 18 mm w. e. yr^{-1} (28%) larger than that during winter–summer period. The seasonality of SMB in the EGRIP area is the opposite of that in the NEEM area (Kuramoto et al., 2011). The different seasonality in those areas may reflect the difference in water vapor source.

Declaration of competing interest

The authors declare that they have no known competing financial interests or personal relationships that could have appeared to influence the work reported in this paper.

Acknowledgements

References

Anklin, M., Stauffer, B., 1994. Pattern of annual snow accumulation along a west Greenland flow lone: no significant change observed during recent decades, 1994. Tellus B 46 (4), 294–303. https://doi.org/10.3402/tellusb.v46i4.15804.

Bales, R.C., McConnell, J.R., Mosley-Thompson, E., Csatho, B., 2001. Accumulation over the Greenland ice sheet from historical and recent records. J. Geophys. Res. 106 (D24) https://doi.org/10.1029/2001JD900153.

Beer, J., Finkel, R.C., Bonani, G., Gäggeler, H., Görlach, U., Jacob, P., Klockow, D., Langway Jr., C.C., Neftel, A., Oeschger, H., Schotterer, U., Schwander, J., Siegenthaler, U., Suter, M., Wagenbach, D., Wölfli, W., 1991. Seasonal variations in the concentrations of 10Be, Cl–, NO3–, SO42–, H2O2, 210Pb, 3H mineral dust and δ18O in Greenland snow. Atmos. Environ. 25 (5–6), 899–904.

Bintanja, R., Selten, F.M., 2014. Future increases in Arctic precipitation linked to local evaporation and sea-ice retreat. Nature 509, 479–482. https://doi.org/10.1038/nature13259.

Buchardt, S.L., Clausen, H.B., Vinther, B.M., Dahl-Jensen, D., 2012. Investigating the past and recent δ18O-accumulation relationship seen in Greenland ice cores. Clim. Past 8, 2053–2059. https://doi.org/10.5194/cp-8-2053-2012.

Castellani, B.B., Shupe, M.D., Hudak, D.R., Sheppard, B.E., 2015. The annual cycle of snowfall at Summit, Greenland. J. Geophys. Res. Atmos. 120, 6654–6668. https://doi.org/10.1002/2015JD023072.

Dansgaard, W., 1973. Stable isotope glaciology. Medd. Groenl. 197 (2), 1–53.

Fettweis, X., Box, J.E., Agosta, C., Amory, C., Kittel, C., Lang, C., van As, D., Machguth, H., Gallée, H., 2017. Reconstructions of the 1900-2015 Greenland ice sheet surface mass balance using the regional climate MAR model. Cryosphere 11, 1015–1033. https://doi.org/10.5194/tc-11-1015-2017.

Finkel, R.C., Langway Jr., C.C., Clausen, H.B., 1986. Changes in precipitation chemistry at Dye 3, Greenland. J. Geophys. Res. 91 (D9), 9849–9855.

Fischer, H., Wagenbach, D., Kipfstuhl, J., 1998a. Sulfate and nitrate firn concentrations on the Greenland ice sheet: 1. Large-scale geographical deposition changes. J. Geophys. Res. 103 (D17), 21927–21934.

Fischer, H., Wagenbach, D., Kipfstuhl, J., 1998b. Sulfate and nitrate firn concentrations on the Greenland ice sheet: 2. Temporal anthropogenic deposition changes. J. Geophys. Res. 103 (D17), 21935–21942.

Gfeller, G., Fischer, H., Bigler, M., Schüpbach, S., Leuenberger, D., Mini, O., 2014. Representativeness and seasonality of major ion records derived from NEEM firn cores. Cryosphere 8 (5), 1855–1870. https://doi.org/10.5194/tc-8-1855-2014.

Hawley, R.L., Courville, Z.R., Kehrl, L.M., Lutz, E.R., Osterberg, E.C., Overly, T.B., Wong, G.J., 2014. Recent accumulation variability in northwest Greenland from ground-penetrating radar and shallow cores along the Greenland Inland Traverse. J. Glaciol. 60 (220), 375–382.

Johnsen, S.J., Dansgaard, W., Clausen, S.J., Langway, C.C., 1972. Oxygen isotope profiles through the Antarctic and Greenland ice sheets. Nature 235, 429–434.

Johnsen, S.J., Dansgaard, W., White, J.W.C., 1989. The origin of Arctic precipitation under present and glacial conditions. Tellus B 41 (4), 452–468.

Kopec, B.G., Feng, X., Michel, F.A., Posmentier, E.S., 2016. Influence of sea ice on Arctic precipitation. P. Natl. Acad. Sci. 113, 46–51. https://doi.org/10.1073/pnas.1504633113.

Koyama, T., Stroeve, J., 2019. Greenland monthly precipitation analysis from the Arctic System Reanalysis (ASR): 2000–2012. Polar Science 19, 1–12. https://doi.org/10.1016/j.polar.2018.09.001.

Kuramoto, T., Goto-Azuma, K., Hirabayashi, M., Miyake, T., Motoyama, H., Dahl-Jensen, D., Steffensen, J.P., 2011. Seasonal variations of snow chemistry at NEEM, Greenland. Ann. Glaciol. 52 (58), 93–200. https://doi.org/10.3189/172756411797252365.

Langen, P.L., Fausto, R.S., Vandecrux, B., Mottram, R.H., Box, J.E., 2017. Liquid water flow and retention on the Greenland Ice Sheet in the regional climate model HIRHAM5: local and large-scale impacts. Front. Earth Sci. 4, 110. https://doi.org/10.3389/feart.2016.00110.

Legrand, M., Mayewski, P., 1997. Glaciochemistry of Polar ice cores: a review. Rev. Geophys. 35, 219–243. https://doi.org/10.1029/96RG03527.

Nakazawa, F., Nagatsuka, N., Hirabayashi, M., Goto-Azuma, K., Steffensen, J.P., Dahl-Jensen, D., 2020. Variation in recent annual snow deposition and seasonality of snow chemistry at the East Greenland Ice Core Project (EGRIP) camp, Greenland. Polar Science. Submitted for publication.

Niwano, M., Aoki, T., Hashimoto, A., Matoba, S., Yamaguchi, S., Tanikawa, T., Fujita, K., Tsushima, A., Iizuka, Y., Shimada, R., Hori, M., 2018. NHM-SMAP: spatially and temporally high-resolution nonhydrostatic atmospheric model coupled with detailed snow process model for Greenland Ice Sheet. Cryosphere 12, 635–655. https://doi.org/10.5194/tc-12-635-2018.

Noël, B., van de Berg, W.J., van Meijgaard, E., Kuipers Munneke, P., van de Wal, R.S.W., van den Broeke, M.R., 2015. Evaluation of the updated regional climate model RACMO2.3: summer snowfall impact on the Greenland Ice Sheet. Cryosphere 9, 1831–1844. https://doi.org/10.5194/tc-9-1831-2015.

Nusbaumer, J., Alexander, P.M., LeGrande, A.N., Tedesco, M., 2019. Spatial shift of Greenland moisture sources related to enhanced Arctic warming. Geophys. Res. Lett. 46 https://doi.org/10.1029/2019GL084633.

Ohmura, A., Reeh, N., 1991. New precipitation and accumulation maps for Greenland. J. Glaciol. 37 (125), 140–148. https://doi.org/10.3189/S0022143000042891.

Rignot, E., Velicogna, I., van den Broeke, M.R., Monaghan, A., Lenaerts, J., 2011. Acceleration of the contribution of the Greenland and Antarctic ice sheets to sea level rise. Geophys. Res. Lett. 38 (5) https://doi.org/10.1029/2011GL046583.

Shepherd, A., Ivins, E.R., Geruo, A., Barletta, V.R., Bentley, M.J., Bettadpur, S., Briggs, K. H., Bromwich, D.H., Forsberg, R., Galin, N., Horwath, M., Jacobs, S., Joughin, I., King, M.A., Lenaerts, J.T.M., Li, J.L., Ligtenberg, S.R.M., Luckman, A., Luthcke, S.B., McMillan, M., Meister, R., Milne, G., Mouginot, J., Muir, A., Nicolas, J.P., Paden, J., Payne, A.J., Pritchard, H., Rignot, E., Rott, H., Sorensen, L.S., Scambos, T.A., Scheuchl, B., Schrama, E.J.O., Smith, B., Sundal, A.V., van Angelen, J.H., van den Berg, W.J., van den Broeke, M.R., Vaughan, D.G., Velicogna, I., Wahr, J., Whitehouse, P.L., Wingham, D.J., Yi, D.H., Young, D., Zwally, H.J., 2012. A reconciled estimate of ice-sheet mass balance. Science 338 (6111), 1183–1189. https://doi.org/10.1126/science.1228102.

Steffen, K., Box, J., 2001. Surface climatology of the Greenland ice sheet: Greenland climate network 1995–1999. J. Geophys. Res. 106 (D24), 33951–33964.

Steffensen, J.P., 1985. Microparticles in snow from the South Greenland ice sheet. Tellus 37B (4–5), 286–295.

Uemura, R., Yoshida, N., Kurita, N., Nakawo, M., Watanabe, O., 2004. An observation-based method for reconstructing ocean surface changes using a 340,000-year deuterium excess record from the Dome Fuji ice core. Antarctica. Geophys. Res. Lett. 31 (13), L13216. https://doi.org/10.1029/2004GL019954.

Uemura, R., 2007. Studies on the reconstruction of past temperature changes from stable isotopes of water: records of millennialscale climate change from polar ice cores. Quat. Res. (Japan) 46 (2), 147–164. In Japanese with English summary.

Zhang, X., He, J., Zhang, J., Polaykov, I., Gerdes, R., Inoue, J., Wu, P., 2013. Enhanced poleward moisture transport and amplified northern high-latitude wetting trend. Nat. Clim. Change 3 (1), 47–51. https://doi.org/10.1038/nclimate1631.